

Taming plasmonic nanocavities for subradiant entanglement

Angus Crookes¹, Ben Yuen¹, and Angela Demetriadou^{*1}

¹*School of Physics and Astronomy, University of Birmingham, Edgbaston, Birmingham, B15 2TT, United Kingdom*

October 8, 2024

Abstract

Recent rapid advances in quantum nanoplasmonics offer the potential for accessing quantum phenomena at room temperature. Despite this, entangled states have not yet been realised, and remain an outstanding challenge. In this work, we demonstrate how entanglement emerges in plasmonic nanocavities, which are inherently multi-mode, and demonstrate the conditions necessary for entanglement to persist. We find that, in general, these conditions are broken due to coupling with multiple plasmonic modes of different parity. We address this challenge with a new nanocavity design that supports high selective coupling to a single mode, enabling the robust generation of subradiant entanglement in nanoplasmonics. Our results open exciting prospects for leveraging simple plasmonic setups in ambient

^{*}a.demetriadou@bham.ac.uk

conditions for applications in quantum communication, sensing and rapid quantum memories.

Introduction

Quantum entanglement plays an indispensable role in various fields of quantum information, including quantum computation [1], cryptography [2, 3], metrology [4] and quantum teleportation [5]. Inspired by these many applications, quantum devices have seen rapid progression over the past decade, where research has developed a myriad of high fidelity qubits that can be coherently controlled and initialised [6, 7, 8]. In fact, entanglement across a wide range of platforms has already been achieved [9], such as with trapped ion qubits [10, 11], photon pairs [12, 13, 14], through utilizing cold atoms [15], and between superconducting qubits [16, 17]. However, despite the wide variety of platforms, most have complicated and large setups that operate at cryogenic temperatures to maintain high coherence times and entanglement [18, 19].

In contrast, plasmonic nanocavities have enabled the exploration of quantum phenomena at ambient conditions, due to their unprecedented ability to confine light [20, 21, 22, 23, 24]. Furthermore, their small scale (~ 80 nm) has the potential for high density integration into nanoscale devices and the ability to harness chemical processes at the single molecule level [25]. Plasmonic nanocavities are also easy to synthesise, and are chemically robust, making experiments reliable and highly reproducible [26, 27, 28, 29]. Hence, several studies have demonstrated single molecule strong coupling at room temperature [30, 31, 26, 27], which provides a potential avenue for entanglement. Despite this, entangled states have not yet been realised with nanoplasmonics and remains an outstanding challenge.

In this work, we demonstrate how entanglement in realistic, multi-mode plasmonic nanocavities emerges via the plasmonic loss, and obtain the general conditions for its persistence. We show why these conditions are not met in conventional plasmonic systems, since the quantum emitters (QEs) couple to multiple modes that have different parity and relative coupling strengths. To address these challenges, we present a unique, easily realizable plasmonic nanocavity that suppresses the influence of multiple modes on entanglement by isolating a single even mode that is strongly coupled to the QEs. In this new design, we demonstrate the robust generation of subradiant entanglement via plasmonic loss, which is irrespective of QE placement. Our results open exciting prospects for generating entanglement at room temperature with simple plasmonic setups.

Results and discussion

Creating stable quantum entanglement in plasmonic systems is extremely challenging, as unavoidable plasmonic losses such as Ohmic heating and radiation, result in the loss of quantum coherence. However, cavity dissipation can also be used to drive QEs into entangled states [32, 33, 34, 35, 36, 37, 38, 39]. The central idea is to prepare two QEs in a superposition state, where one part evolves through interaction with the plasmonic cavity, while the other part is protected from cavity dissipation and is persistent.

This population trapping mechanism is particularly successful when the QEs are subject to strong field enhancements and large cavity losses, as this increases the rate of entanglement formation. Therefore, recent research has focused on entanglement within nanoparticle on mirror (NPoM) cavities, which are easy to synthesise, very robust, and provide extremely small mode volumes that bring the system into the strong coupling regime at room temperature [30, 37, 39]. A

schematic of the NPoM system is shown in Fig. 1a in which both QEs are prepared in the initial state $|e, g\rangle = \frac{1}{\sqrt{2}}(|\psi_-\rangle + |\psi_+\rangle)$, where $|\psi_\pm\rangle = \frac{1}{\sqrt{2}}(|e, g\rangle \pm |g, e\rangle)$ are both entangled states, yet $|e, g\rangle$ is not. In previous studies [39, 37], it is assumed that only a single plasmonic mode is interacting with the QEs, which is a common approximation in quantum plasmonics. For the single mode case, they demonstrated that when the coupling of the QEs to the plasmonic mode is identical, $|\psi_+\rangle$ exchanges energy with the cavity mode and decays through plasmonic dissipation, while $|\psi_-\rangle$ is decoupled from the cavity (i.e. is subradiant), which remains to form a persistent entangled state.

However, in reality plasmonic systems feature multiple dissipative and broadband modes that all couple strongly to the QEs in the nanocavity, even if the modes are off-resonant [40, 41, 42, 43]. In this work, we explicitly describe the interaction between multiple plasmonic modes and two QEs using an open quantum system formalism, where the density operator ρ evolves under:

$$\dot{\rho}(t) = -i[\mathcal{H}_{\text{sys}}, \rho] + \sum_{\xi}^N \kappa_{\xi} \left(a_{\xi} \rho a_{\xi}^{\dagger} - \frac{1}{2} \{a_{\xi}^{\dagger} a_{\xi}, \rho\} \right) \quad (1)$$

with

$$\mathcal{H} = \sum_{\xi=1}^N \omega_{\xi} a_{\xi}^{\dagger} a_{\xi} + \sum_{j=1}^M \frac{\omega_e}{2} \sigma_z^j + \sum_{\xi,j}^{N,M} g_{\xi}(\mathbf{r}_j) a_{\xi}^{\dagger} \sigma_j + g_{\xi}^*(\mathbf{r}_j) a_{\xi} \sigma_j^{\dagger} \quad (2)$$

where a_{ξ}^{\dagger} and a_{ξ} are the creation and annihilation operators for each plasmonic mode ξ with frequency ω_{ξ} and loss rate κ_{ξ} and σ_j^{\dagger} and σ_j are the raising and lowering operators for a QE with transition frequency ω_e . In addition, the position dependent coupling strength between mode ξ and quantum emitter j at \mathbf{r}_j is given by $g_{\xi}(\mathbf{r}_j) = g_{\xi j} e^{i\phi_{\xi j}}$, which is separated into its magnitude, $g_{\xi j}$ and phase, $\phi_{\xi j}$.

For such multi-mode systems, the population trapping mechanism is satisfied when a dark (subradiant) state $|\psi_{\text{D}}\rangle = \cos \theta |e, g\rangle + e^{i\chi} \sin \theta |g, e\rangle$ is decoupled from the cavity and a bright (super-radiant) state $|\psi_{\text{B}}\rangle = -e^{i\chi} \sin \theta |e, g\rangle + \cos \theta |g, e\rangle$

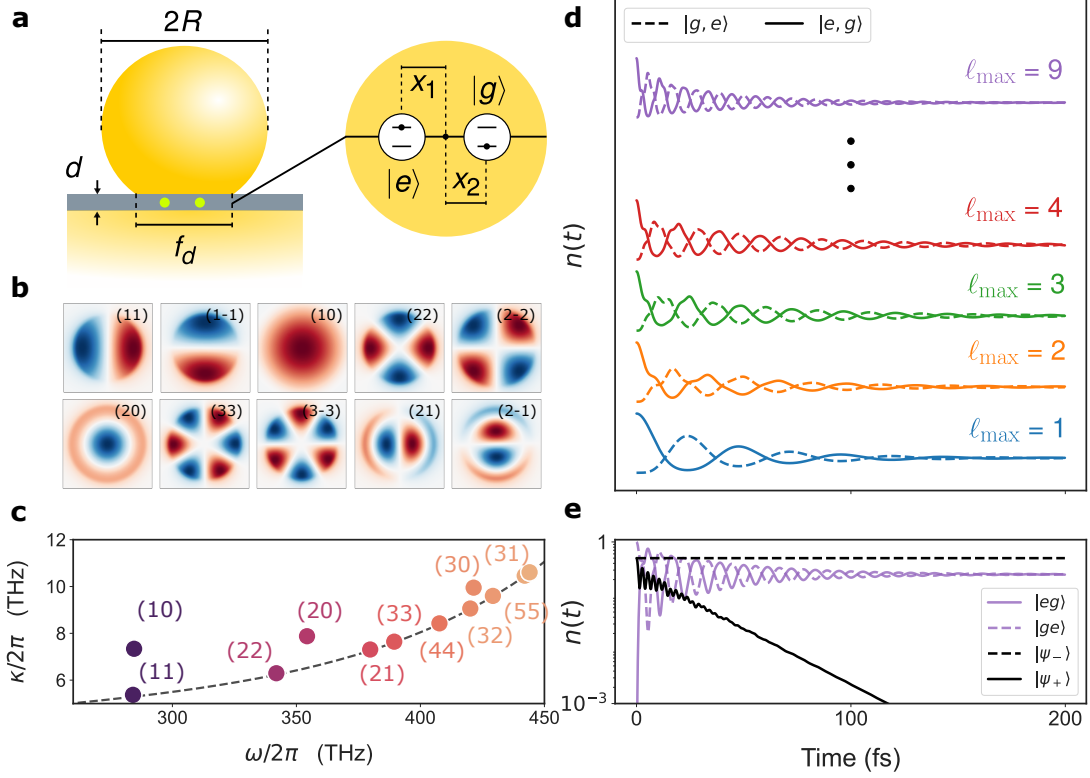


Figure 1: **Entanglement formation in nanoparticle on mirror cavities.** **a** Schematic of a gold nanoparticle on mirror (NPoM) cavity with radius $R = 40$ nm, facet diameter $f_d = 16$ nm, gap spacing $d_{\text{gap}} = 1$ nm, and gap permittivity $n_{\text{gap}} = 2.5$. The cavity is loaded with two quantum emitters at the centre of the nano-gap at position x_1 and x_2 respectively. **b** Electric field, $E_z(x, y, 0)$, of the first fifteen quasinormal modes (QNM's) supported by the bare cavity. **c** Complex representation of the QNM eigenvalues, $\tilde{\omega}_\xi = \omega_\xi - \frac{i\kappa_\xi}{2}$, with respect to the eigenvalues of a metal-insulator-metal waveguide (black-dashed line). **d** Population of each QE's excited state (solid - $|e, g\rangle$ and dashed - $|g, e\rangle$) as a function of time at $x_1 = x_2 = 0$. The interaction with off-resonant plasmonic modes increases the oscillation frequency but despite this always forms the entangled subradiant state, $|\psi_-\rangle = \frac{1}{\sqrt{2}}(|e, g\rangle - |g, e\rangle)$. **e** Population of each quantum emitters excited state and of the entangled states $|\psi_-\rangle$ and $|\psi_+\rangle$ for the case of $\ell_{\text{max}} = 9$ and $x_1 = x_2 = 0$.

decays rapidly, where $\theta \in [-\pi/2, \pi/2]$ and $\chi \in [0, 2\pi]$. The state $|\psi_D\rangle$ is dark (and therefore persistent) under the conditions:

$$\left(\frac{g_{\xi 1}}{g_{\xi 2}}\right) e^{i(\phi_{\xi 1} - \phi_{\xi 2})} = -e^{i\chi} \tan \theta \quad \text{for all modes } \xi \quad (3)$$

which is valid (but not necessarily satisfied) for any dissipative multi-mode cavity, and depends on the magnitude and phase of the QEs' coupling strengths to each mode in the cavity (see Methods for more details). Therefore, the initial state $|e, g\rangle = \cos \theta |\psi_D\rangle - e^{i\chi} \sin \theta |\psi_B\rangle$ that is considered here, generates the persistent entangled state $|\psi_D\rangle$ only when Eq. (3) is satisfied.

To assess the entanglement capabilities of commonly used plasmonic systems using equation 3, we consider the NPoM configuration and calculate its multiple modes. We obtain their frequencies, loss rates, and interaction strengths using the auxiliary eigenvalue method [44, 45, 46]. Here, eigenstates of the bare cavity are expressed as quasinormal modes (QNMs) that have a finite lifetime given by their complex eigenfrequency $\tilde{\omega}_\xi = \omega_\xi - i\frac{\kappa_\xi}{2}$, where ω_ξ and κ_ξ are the resonant frequency and decay-rate corresponding to each mode with electric and magnetic fields $\tilde{\mathbf{E}}_\xi(\mathbf{r})$ and $\tilde{\mathbf{H}}_\xi(\mathbf{r})$. From these fields, one can obtain the coupling strength of each QNM ξ to each QE j as: $g_{\xi j} e^{i\phi_{\xi j}} = \sqrt{\frac{\omega_\xi}{\hbar V_\xi}} \boldsymbol{\mu} \cdot \tilde{\mathbf{E}}_\xi(\mathbf{r}_j)$ where $\boldsymbol{\mu}$ is the QE dipole moment and $V_\xi = \iiint_\Omega \left[\tilde{\mathbf{E}} \cdot \frac{\partial \omega_\xi}{\partial \omega} \tilde{\mathbf{E}} - \mu_0 \tilde{\mathbf{H}} \cdot \frac{\partial \omega_\xi}{\partial \omega} \tilde{\mathbf{H}} \right] dV$ is the QNM normalisation factor. The electric field, $\tilde{E}_z^\xi(x, y, 0)$, of the first ten QNMs at the centre of the nanocavity are shown in Fig. 1b., each characterised by an index $\xi = (lm)$, where $l \in \mathbb{Z}^+$ is the number of radial anti-nodes and $-l \leq m \leq l$ the pairs of azimuthal anti-nodes [47]. The $m = 0$ modes are cylindrically symmetric and have a node at the nanocavity centre, while the $m \neq 0$ modes are degenerate with an orthogonal $m, -m$ pair, and have an anti-node at the nanocavity centre. Importantly, the value of $|m|$ defines the modes parity, with $|m| = 0, 2, 4, 6, \dots$ for even and $|m| = 1, 3, 5, 7, \dots$ for odd modes respectively [47, 48]. The complex eigenfrequencies associated with each QNM are displayed in Fig. 1c. In this system, all $m \neq 0$ modes predominantly

lose energy via ohmic heating, since they closely follow the eigenvalues of a metal-insulator-metal waveguide (i.e. dashed line) [47] while all $m = 0$ modes have an additional radiative loss (see Supplementary Information for details on the calculation). The parameters κ_ξ , ω_ξ , and $g_{\xi j}e^{i\phi_{\xi j}}$ are obtained from the mode decomposition for the first 103 modes up to $\xi = (90)$, which allows us to assess the impact of the multiple modes on the entanglement.

The entanglement conditions described by equation (3) are always satisfied for two QEs at the same position within the nanocavity, as both QEs have identical coupling strengths and phases ($g_{\xi 1} = g_{\xi 2}$ and $\phi_{\xi 1} = \phi_{\xi 2}$) for each mode ξ . Therefore, in this case the system always exhibits persistent entanglement irrespective of the number of interacting modes, as the state $|\psi_-\rangle$ is always dark. This is demonstrated numerically in Fig. 1d where we consider two QEs at the nanocavity centre i.e. $x_1 = x_2 = 0$, with transition frequency $\omega_e = \omega_{(10)} = 283$ THz and dipole moment $\mu_0 = 1 \times 10^{-28}$ Cm. Here, we calculate the time evolution including interacting modes up to $(\ell_{\max}0)$ for various values of the index ℓ_{\max} where only $m = 0$ modes contribute, since all $m \neq 0$ modes vanish at the centre ($x = y = 0$). For all values of ℓ_{\max} , the two QEs remain correlated with one another, and without exception relax to the same subradiant entangled state $|\psi_-\rangle$ with steady state density matrix $\rho_{\text{ss}} = \frac{1}{2}|g, g\rangle\langle g, g| + \frac{1}{2}|\psi_-\rangle\langle\psi_-|$. This is shown for the specific case $\ell_{\max} = 9$ in Fig. 1e from which it is clear that the population of $|\psi_-\rangle$ does not change, and is therefore decoupled from the cavity. This is consistent with the single mode approximation ($\ell_{\max} = 1$), with now more rapid oscillations between the two QEs as we include off-resonant modes. This highlights that multiple lossy modes do not prevent the formation of entanglement in plasmonic systems, provided the conditions in Eq (3) are satisfied.

Whilst this example clearly shows persistent entanglement in a multi-mode plasmonic nanocavity, in reality two QEs cannot be located at the exact same

position. To guarantee that the magnitude of both QEs' coupling strengths to each mode still satisfies Eq. (3), we first place them symmetrically away from the centre of the nanocavity (i.e. $x_2 = -x_1$ and $g_{\xi 1} = g_{\xi 2}$) such that the phase $\phi_{\xi j}$ of the coupling strength becomes the deciding factor on entanglement. In this case, when $x_1 = -x_2 \neq 0$, a more expansive set of modes (i.e. $m \neq 0$) that can have different parities now couple to both QEs. Since Eq (3) shows that persistence of entanglement is dependent on the mode parity ($\phi_{\xi 1}, \phi_{\xi 2}$), we consider three situations where we include only: (1) even modes, (2) odd modes and (3) all modes coupled to the QEs as shown in Fig. 2.

To better quantify the entanglement for any position of the QEs in the nanocavity, we use the Wootters concurrence [49, 50]:

$$C(\rho) = \max(0, \lambda_1 - \lambda_2 - \lambda_3 - \lambda_4) \quad (4)$$

where $\{\lambda_i\}$ is the set of ordered eigenvalues of $R = \sqrt{\sqrt{\rho}\tilde{\rho}\sqrt{\rho}}$ and $\tilde{\rho} = \sigma_y \otimes \sigma_y \rho^* \sigma_y \otimes \sigma_y$ is the spin flipped reduced density matrix. The entanglement between both QEs is then determined by performing a partial trace over the plasmonic degrees of freedom and calculating the concurrence on the remaining reduced density matrix. In this way, a maximally entangled state is given by a concurrence of unity while a completely separable state causes the concurrence to vanish. Fig. 2 a. shows the entanglement when only even plasmonic modes ($m = 0, 2, 4, \dots$) are coupled with the QEs; the resulting steady state remains entangled due to a population of the state $|\psi_-\rangle$. In Fig. 2b only odd modes ($m = 1, 3, 5, \dots$) are coupled to the QEs, which again results in a steady state that exhibits entanglement but now due to a population of the state $|\psi_+\rangle$. In this system, when $x_1 = -x_2$ and therefore $g_{\xi 1} = g_{\xi 2}$, the conditions for persistent entanglement due to population of the dark state $|\psi_D\rangle$ described in Eq. (3) can be reduced to:

$$e^{i\chi} = -e^{i(\phi_{\xi 1} - \phi_{\xi 2})}, \quad (5)$$

with $\theta = \pi/4$, which must be satisfied for all modes independently for entanglement to emerge. It is clear from Eq. (5) that the solutions (1) $\chi = \pi$ is satisfied when all the nanocavity modes are even since $\phi_{\xi_1} - \phi_{\xi_2} = 0$ and (2) $\chi = 0$ is satisfied when all the modes in the nanocavity are odd, since $\phi_{\xi_1} - \phi_{\xi_2} = \pi$. In each case, the corresponding entangled state protected from dissipation is switched from $|\psi_{-}\rangle$ for even modes to $|\psi_{+}\rangle$ for odd modes, as seen in the top panels of Fig 2a-b.

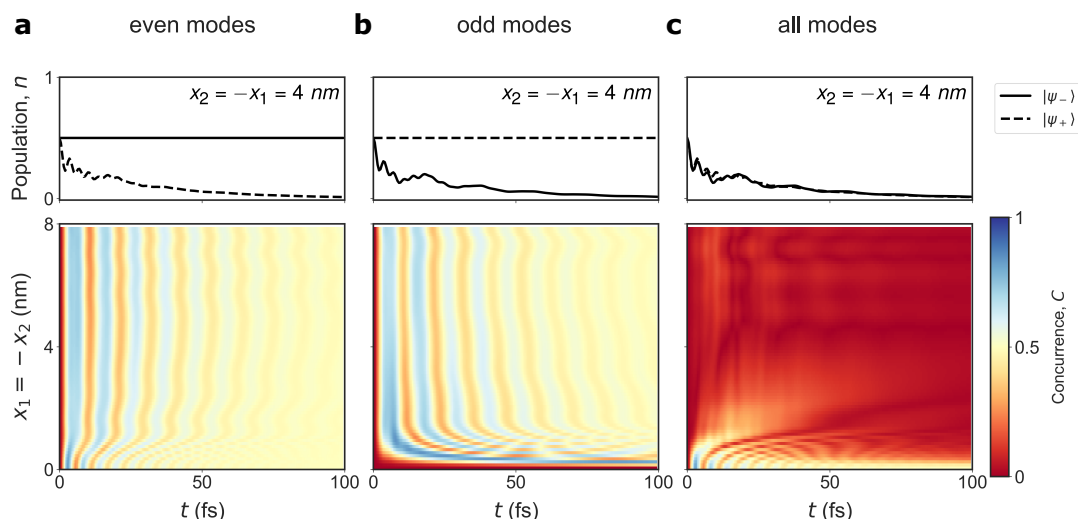


Figure 2: **Effect of mode parity on sub-radiant entanglement.** **a-c** Concurrence as a function of symmetric displacement of both quantum emitters (i.e. $x_1 = -x_2$) including only: **a** even plasmonic modes ($m = 0, 2, 4, \dots$) **b** odd plasmonic modes ($m = 1, 3, 5, \dots$) and **c** all modes ($m = 0, 1, 2, 3, \dots$) in the interaction. The corresponding populations of both entangled states $|\psi_{-}\rangle$ and $|\psi_{+}\rangle$ are also shown at a displacement of $x_2 = -x_1 = 4$ nm, demonstrating a clear switching between the entangled subradiant states for even and odd modes respectively. No persistent entanglement is observed with both even and odd modes.

If both QEs are strongly coupled to a combination of even and odd modes, then

the persistence conditions in Eq. (5) are not satisfied, and no entanglement is observed at long times. Fig. 2c shows exactly this - when the complete collection of plasmonic modes is included (both even and odd modes) there is a complete loss of entanglement, with C vanishing for all $x_1 = -x_2 > 0.5$ nm. This is emphasised in the top panel, showing both populations of $|\psi_-\rangle$ and $|\psi_+\rangle$ decay at $x_2 = -x_1 = 4$ nm. In addition, we so far considered symmetric QE placement to ensure that $g_{\xi 1} = g_{\xi 2}$. However, if the ratio $g_{\xi 1}/g_{\xi 2}$ is different for each mode ξ , which is the case for asymmetric QE placement, then entanglement is also completely removed. This is because the persistence conditions in Eq. (3) are not satisfied for asymmetric QE placement in most plasmonic nanocavities (see Supplementary Information). Hence, both the relative coupling strengths of the two QEs to each mode, as well as the mode parity, dominate the formation of subradiant entangled states in multi-mode cavities. This presents a major challenge in the generation of entanglement within plasmonic nanocavities, where modes of different parity and strong field enhancements, almost always co-exist.

Taming plasmonic systems for entanglement

To overcome this problem, one needs to design plasmonic nanocavities where the system favours either even or odd modes in a certain spatial region to place the QEs. To achieve this, we introduce a new design that fulfils this parity selection. A schematic of our new design is shown in Fig. 3a, where we consider the same nanoparticle-on-mirror, but now with a hollow cylinder of radius $r = 10$ nm and height $h = 3$ nm etched into the nanoparticle facet of size $f_d = 30$ nm. The z -component of the electric field of each QNM, $\tilde{E}_z^\xi(x, y, z = (d_{\text{gap}} + h)/2)$, is shown inside the hollow cylinder in Fig. 3b. This unique nanocavity design also supports both even and odd modes, but the fields of $m \neq 0$ modes are now concentrated at the edges of the hollow cylinder and have very small coupling strengths inside.

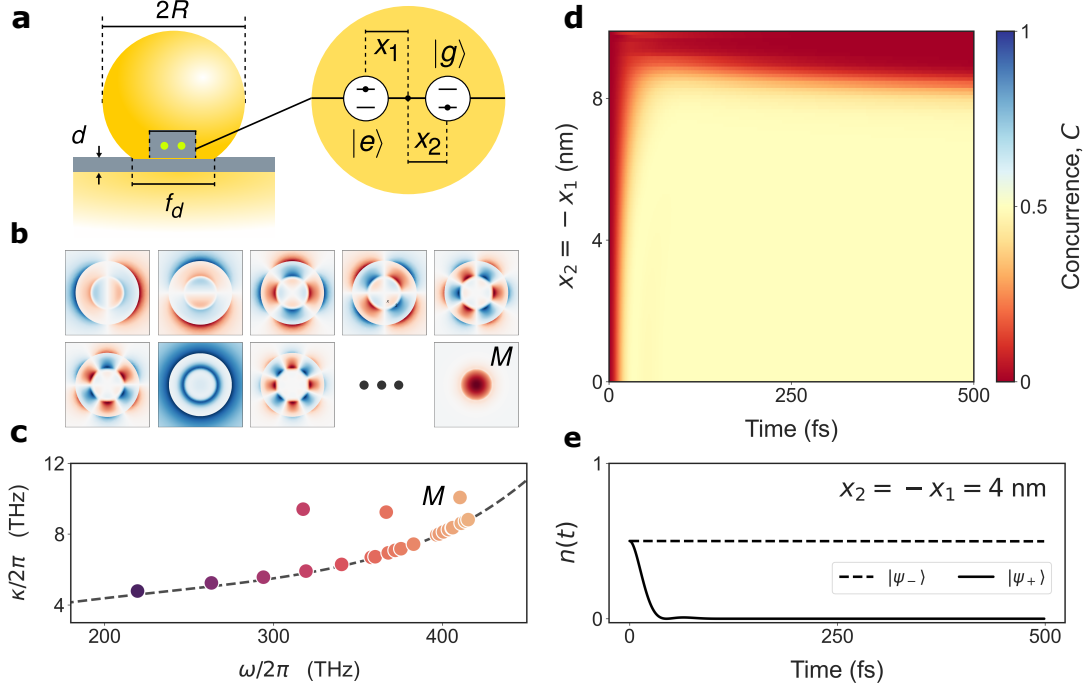


Figure 3: **Plasmonic nanocavity design for robust entanglement** **a** Schematic of a gold nanoparticle on mirror (NPoM) cavity with radius $R = 40$ nm, facet diameter $f_d = 30$ nm, gap spacing $d_{\text{gap}} = 1$ nm, and gap permittivity $n_{\text{gap}} = 2.5$. Into the nanoparticle facet a hollow cylinder is etched, of height $h = 3$ nm and radius $r = 10$ nm. **b** Electric field distribution of quasinormal modes (QNMs) within the perforation at $z = (d_{\text{gap}} + h)/2$. **c** Complex representation of the QNM eigenvalues with respect to those of a metal-insulator-metal waveguide (black-dashed line) **d** Concurrence as a function of time and displacement ($x_2 = -x_1$) of both emitters. **e** Quantum emitter entangled state populations, $|\psi_{-}\rangle$ and $|\psi_{+}\rangle$, highlighted at a displacement of $x_2 = -x_1 = 4$ nm.

Instead, the fields within the cylinder are dominated by a single (even) mode at $\lambda = 730$ nm (labelled M). This mode originates from the cylindrical hollow

geometry and has a field enhancement over an order of magnitude larger than all other modes within this spatial region. The complex eigenfrequencies associated with each QNM are displayed in Fig. 3c and again share close agreement with those obtained from a metal-insulator-metal waveguide (dashed line). Importantly, despite overlapping resonances in the frequency domain, we are able to achieve highly selective coupling of QEs to only mode M by placing them within the hollow cylinder, where the fields of all other modes are suppressed.

The entanglement as a function of time and symmetric placements ($x_2 = -x_1$) at $z = (d_{\text{gap}} + h)/2$ is shown in Fig. 3d-e. where both QEs have dipole moment μ_0 , frequency $\omega_e = \omega_M = 730$ nm and each interacts with 40 plasmonic modes. In this new design, although the persistence conditions in Eq. (3) are not strictly satisfied, the weak coupling of all other modes that violate these conditions are negligible, and thus have little effect on the dynamics over which entanglement emerges. Therefore, this allows for persistent entanglement to emerge for $x_2 = -x_1 \lesssim 8$ nm as a result of the persistence of $|\psi_{-}\rangle$. Beyond 8nm from the centre, other modes become significant due to the high charge confinement on the hollow cylinder walls, which break the entanglement conditions in this region (Fig. 3d). However, this is just 1 – 2 nm away from the metallic wall of the hollow cylinder.

Due to the unique performance of our new nanocavity design, entanglement is actually also persistent even for asymmetric QE positions. Fig. 4a shows the concurrence after a long time has elapsed (i.e. $t = 1$ ps) as a function of both QE positions (x_1 and x_2) considering coupling to 40 plasmonic modes. In contrast to other plasmonic cavities, entanglement is observed at all positions within the hollow cylinder for $x_1, x_2 \lesssim 8$ nm. Entanglement between QEs with asymmetric positions is rarely possible in other nanocavities, because the multi-mode persistence conditions in Eq. (3) are not satisfied when $g_{\xi 1}/g_{\xi 2}$ is different for each mode ξ . Instead, the persistence of entanglement here originates from the strong

coupling of both QEs to a single plasmonic mode, which allows us to safely take a single-mode approximation, within which the steady state density matrix can be expressed as:

$$\rho_{\text{ss}} = \left(1 - \frac{1}{1 + |\alpha|^2}\right) |g, g\rangle\langle g, g| + \frac{1}{1 + |\alpha|^2} |\psi_{\text{D}}\rangle\langle\psi_{\text{D}}| \quad (6)$$

where $|\psi_{\text{D}}\rangle = \frac{1}{\sqrt{1+|\alpha|^2}} (|e, g\rangle - \alpha|g, e\rangle)$ is the (dark) entangled state between both emitters and $\alpha = g_{11}e^{i\phi_{11}}/g_{12}e^{i\phi_{12}}$ is the ratio of coupling strengths between each QE and the spatially isolated plasmonic mode M (see Methods for full details). In this case, there is always a persistent entangled state, which depends on the coupling strengths of both QEs to the plasmonic mode. Note that when the coupling is symmetric (i.e. $\alpha = 1$) Eq (6) reduces to the previous case, where entanglement is due to the state $|\psi_{-}\rangle$.

The single mode approximation provides an excellent description of entanglement within this plasmonic nanocavity for QEs placed within the hollow cylinder. This can be seen in Fig. 4b where the concurrence at $t = 1$ ps is plotted using the single-mode approximation (dashed lines) together with the full calculations (solid lines) for $x_1 = 0$ and $x_2 = 0$ respectively. Furthermore, Eq. 6 also gives a simple explanation for differences in the degree of entanglement which results from the asymmetric initial state $|e, g\rangle$ and two competing forces: (1) population of the entangled state $|\psi_{\text{D}}\rangle$ i.e. $\langle\psi_{\text{D}}|\rho_{\text{ss}}|\psi_{\text{D}}\rangle = \frac{1}{1+|\alpha|^2}$ and (2) closeness (fidelity) of the entangled state $|\psi_{\text{D}}\rangle$ to the maximally entangled state $|\psi_{-}\rangle$ i.e. $F = |\langle\psi_{-}|\psi_{\text{D}}\rangle|^2 = \frac{|1+\alpha|^2}{2(1+|\alpha|^2)}$. When $|\alpha| > 1$ (which corresponds to displacement of the initially unexcited QE away from the centre) the population and fidelity of the entangled state $|\psi_{\text{D}}\rangle$ decreases, leading to a decrease in entanglement. However, when $|\alpha| < 1$ (which corresponds to displacement of the initially excited QE away from the centre) the fidelity of the entangled state also decreases but the population of $|\psi_{\text{D}}\rangle$ increases more rapidly. This produces an initial increase in the overall entanglement of the system before eventually decreasing at larger separations (see

Supplementary Information for more details).

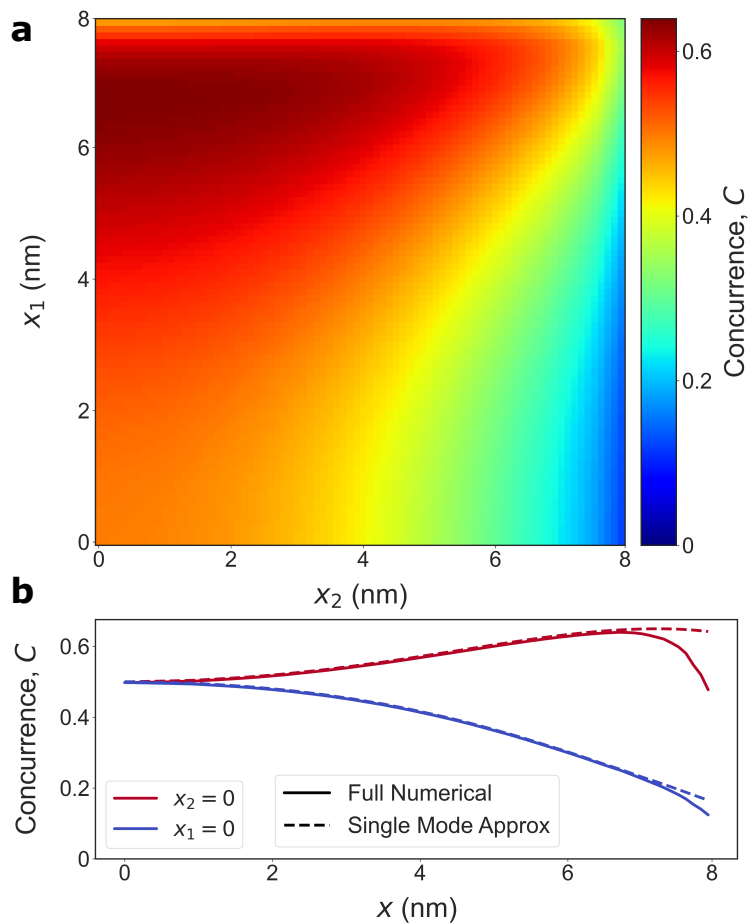


Figure 4: **Entanglement generation under asymmetric displacement.** **a** Concurrence, evaluated at $t = 1$ ps, as a function of asymmetric quantum emitter position, x_1 and x_2 . The QE at x_1 is initially excited. **b** Concurrence, evaluated at $t = 1$ ps, as a function of quantum emitter position for $x_1 = 0$ (blue) and $x_2 = 0$ (red). Calculations are performed using forty modes (solid lines) and a single mode approximation (dashed lines).

Conclusions

In conclusion, our work elucidates the crucial role of mode parity and relative coupling strength on the generation and manipulation of quantum entanglement of two QEs in cavities. We have shown that the presence of multiple dissipative modes does not prevent the persistence of entanglement. Instead, for cavities with multiple modes, such as plasmonic nanocavities, their parity and relative coupling strengths define the persistence or destruction of entangled states. To address this challenge, we design a new plasmonic nanocavity that suppresses coupling of QEs to all but a single dominant mode, enabling the emergence of robust entanglement regardless of the QE placement. Our results pave the way towards the experimental realization of entanglement in plasmonic systems at ambient conditions, and mark a significant step towards practical applications in quantum communications, sensing and rapid quantum memories using nanoplasmonics.

Methods

Multi-mode persistence conditions

In a multi-mode cavity, the state $|\psi_D\rangle = \cos\theta|e, g\rangle + e^{i\chi}\sin\theta|g, e\rangle$ is subradiant if it is decoupled from the cavity. This occurs when it is part of the null-space of the Hamiltonian i.e. $\mathcal{H}|\psi_D\rangle = 0$ which can be expressed as:

$$\mathcal{H}|\psi_D\rangle = \sum_{\xi=1}^N [g_{\xi 1}e^{i\phi_{\xi 1}}\cos\theta + g_{\xi 2}e^{i\phi_{\xi 2}}e^{i\chi}\sin\theta] a_{\xi}^{\dagger}|0\rangle^{\otimes N}|g, g\rangle = \bar{0} \quad (7)$$

where $\bar{0}$ is the null-vector. Importantly, since each term in the sum is independent, the expression in square brackets must vanish for every mode ξ that is coupled to the QEs. Applying this requirement gives Eq. (3).

Single-mode approximation

Let an arbitrary state between two quantum emitters be described by the state vector $|\psi_D\rangle = a|e, g\rangle + b|g, e\rangle$. If we require $\mathcal{H}|\psi_D\rangle = 0$ then

$$\mathcal{H}|\psi_D\rangle = \sum_{\xi=1}^N [ag_{\xi 1}e^{i\phi_{\xi 1}} + bg_{\xi 2}e^{i\phi_{\xi 2}}] a_{\xi}^{\dagger}|0\rangle^{\otimes N}|g, g\rangle = 0 \quad (8)$$

where $g_{\xi, j}$ is the magnitude of the coupling strength between mode ξ and atom j and $\phi_{\xi j}$ the corresponding phase. In particular, under a single mode approximation we can derive a state that is always part of the null-space of \mathcal{H} such that $|\psi_D\rangle \in \{|\psi\rangle \mid \mathcal{H}|\psi\rangle = 0\}$ and

$$|\psi_D\rangle = \frac{1}{\sqrt{N}} (|e, g\rangle - \alpha|g, e\rangle) \quad (9)$$

where $\alpha = \frac{g_{11}e^{i\phi_{11}}}{g_{12}e^{i\phi_{12}}}$ and $\tilde{N} = 1 + |\alpha|^2$. Orthonormal to $|\psi_D\rangle$ is the state $|\psi_B\rangle = \frac{1}{\sqrt{1+1/|\alpha|^2}} (|e, g\rangle + \frac{1}{\alpha^*}|g, e\rangle)$ where $\mathcal{H}|\psi_B\rangle \neq 0$. If the system is initialised in an asymmetric state $|e, g\rangle$ then by transforming to the basis $\{|\psi_D\rangle, |\psi_B\rangle\}$ we get:

$$|e, g\rangle = \frac{1}{\sqrt{1 + |\alpha|^2}} |\psi_s\rangle + \frac{1}{\sqrt{1 + \frac{1}{|\alpha|^2}}} |\psi_d\rangle \quad (10)$$

of which part, the $|\psi_D\rangle$ component, is protected from dissipation, while the $|\psi_B\rangle$ component eventually decays to the ground state through plasmonic loss. Therefore, the general steady state density matrix of two quantum emitters interacting with a single mode plasmonic cavity can be written as:

$$\rho_{ss} = \left(1 - \frac{1}{1 + |\alpha|^2}\right) |g, g\rangle\langle g, g| + \frac{1}{1 + |\alpha|^2} |\psi_D\rangle\langle\psi_D| \quad (11)$$

where α encodes the coupling of each quantum emitter to a single plasmonic mode at any position within the nano-cavity (for more details see Supplementary Information).

References

- [1] Michael A Nielsen and Isaac L Chuang. *Quantum computation and quantum information*. Cambridge university press, 2010.
- [2] Nicolas Gisin, Grégoire Ribordy, Wolfgang Tittel, and Hugo Zbinden. Quantum cryptography. *Reviews of modern physics*, 74(1):145, 2002.
- [3] Stefano Pirandola, Ulrik L Andersen, Leonardo Banchi, Mario Berta, Darius Bunandar, Roger Colbeck, Dirk Englund, Tobias Gehring, Cosmo Lupu, Carlo

- Ottaviani, et al. Advances in quantum cryptography. *Advances in optics and photonics*, 12(4):1012–1236, 2020.
- [4] Vittorio Giovannetti, Seth Lloyd, and Lorenzo Maccone. Advances in quantum metrology. *Nature photonics*, 5(4):222–229, 2011.
- [5] Stefano Pirandola, Jens Eisert, Christian Weedbrook, Akira Furusawa, and Samuel L Braunstein. Advances in quantum teleportation. *Nature photonics*, 9(10):641–652, 2015.
- [6] Nicolas Laflorencie. Quantum entanglement in condensed matter systems. *Physics Reports*, 646:1–59, 2016.
- [7] Anasua Chatterjee, Paul Stevenson, Silvano De Franceschi, Andrea Morello, Nathalie P de Leon, and Ferdinand Kuemmeth. Semiconductor qubits in practice. *Nature Reviews Physics*, 3(3):157–177, 2021.
- [8] Göran Wendin. Quantum information processing with superconducting circuits: a review. *Reports on Progress in Physics*, 80(10):106001, 2017.
- [9] Nicolai Friis, Giuseppe Vitagliano, Mehul Malik, and Marcus Huber. Entanglement certification from theory to experiment. *Nature Reviews Physics*, 1(1):72–87, 2019.
- [10] QA Turchette, CS Wood, BE King, CJ Myatt, D Leibfried, WM Itano, C Monroe, and DJ Wineland. Deterministic entanglement of two trapped ions. *Physical Review Letters*, 81(17):3631, 1998.
- [11] Hartmut Häffner, Wolfgang Hänsel, CF Roos, Jan Benhelm, D Chek-al Kar, M Chwalla, T Körber, UD Rapol, M Riebe, PO Schmidt, et al. Scalable multiparticle entanglement of trapped ions. *Nature*, 438(7068):643–646, 2005.

- [12] Alain Aspect, Philippe Grangier, and Gérard Roger. Experimental realization of einstein-podolsky-rosen-bohm gedankenexperiment: A new violation of bell's inequalities. *Physical review letters*, 49(2):91, 1982.
- [13] Marek Zukowski, Anton Zeilinger, and Harald Weinfurter. Entangling photons radiated by independent pulsed sources a. *Annals of the New York academy of Sciences*, 755(1):91–102, 1995.
- [14] Xi-Lin Wang, Luo-Kan Chen, Wei Li, H-L Huang, Chang Liu, Chao Chen, Y-H Luo, Z-E Su, Dian Wu, Z-D Li, et al. Experimental ten-photon entanglement. *Physical review letters*, 117(21):210502, 2016.
- [15] Bing Yang, Hui Sun, Chun-Jiong Huang, Han-Yi Wang, Youjin Deng, Han-Ning Dai, Zhen-Sheng Yuan, and Jian-Wei Pan. Cooling and entangling ultracold atoms in optical lattices. *Science*, 369(6503):550–553, 2020.
- [16] D Riste, M Dukalski, CA Watson, G De Lange, MJ Tiggelman, Ya M Blanter, Konrad W Lehnert, RN Schouten, and L DiCarlo. Deterministic entanglement of superconducting qubits by parity measurement and feedback. *Nature*, 502(7471):350–354, 2013.
- [17] Matthias Steffen, Markus Ansmann, Radoslaw C Bialczak, Nadav Katz, Erik Lucero, Robert McDermott, Matthew Neeley, Eva Maria Weig, Andrew N Cleland, and John M Martinis. Measurement of the entanglement of two superconducting qubits via state tomography. *Science*, 313(5792):1423–1425, 2006.
- [18] Antonio D Córcoles, Jerry M Chow, Jay M Gambetta, Chad Rigetti, James R Rozen, George A Keefe, Mary Beth Rothwell, Mark B Ketchen, and Matthias Steffen. Protecting superconducting qubits from radiation. *Applied Physics Letters*, 99(18), 2011.

- [19] Chenlu Wang, Xuegang Li, Huikai Xu, Zhiyuan Li, Junhua Wang, Zhen Yang, Zhenyu Mi, Xuehui Liang, Tang Su, Chuhong Yang, et al. Towards practical quantum computers: Transmon qubit with a lifetime approaching 0.5 milliseconds. *npj Quantum Information*, 8(1):3, 2022.
- [20] Mark S Tame, KR McEnery, ŞK Özdemir, Jinhyoung Lee, Stefan A Maier, and MS Kim. Quantum plasmonics. *Nature Physics*, 9(6):329–340, 2013.
- [21] Rocío Sáez-Blázquez, Álvaro Cuartero-González, Johannes Feist, Francisco J García-Vidal, and Antonio I Fernández-Domínguez. Plexcitonic quantum light emission from nanoparticle-on-mirror cavities. *Nano Letters*, 22(6):2365–2373, 2022.
- [22] A Gonzalez-Tudela, Diego Martin-Cano, Esteban Moreno, Luis Martin-Moreno, C Tejedor, and Francisco J Garcia-Vidal. Entanglement of two qubits mediated by one-dimensional plasmonic waveguides. *Physical review letters*, 106(2):020501, 2011.
- [23] Esteban Moreno, FJ García-Vidal, Daniel Erni, J Ignacio Cirac, and Luis Martín-Moreno. Theory of plasmon-assisted transmission of entangled photons. *Physical review letters*, 92(23):236801, 2004.
- [24] Alexander Huck, Stephan Smolka, Peter Lodahl, Anders S Sørensen, Alexandra Boltasseva, Jiri Janousek, and Ulrik L Andersen. Demonstration of quadrature-squeezed surface plasmons in a gold waveguide. *Physical review letters*, 102(24):246802, 2009.
- [25] Emiliano Cortés, Lucas V Besteiro, Alessandro Alabastri, Andrea Baldi, Giulia Tagliabue, Angela Demetriadou, and Prineha Narang. Challenges in plasmonic catalysis. *ACS nano*, 14(12):16202–16219, 2020.

- [26] Sabrina Simoncelli, Eva-Maria Roller, Patrick Urban, Robert Schreiber, Andrew J Turberfield, Tim Liedl, and Theobald Lohmuller. Quantitative single-molecule surface-enhanced raman scattering by optothermal tuning of dna origami-assembled plasmonic nanoantennas. *ACS nano*, 10(11):9809–9815, 2016.
- [27] Rohit Chikkaraddy, VA Turek, Nuttawut Kongsuwan, Felix Benz, Cloudy Carnegie, Tim Van De Goor, Bart De Nijs, Angela Demetriadou, Ortwin Hess, Ulrich F Keyser, et al. Mapping nanoscale hotspots with single-molecule emitters assembled into plasmonic nanocavities using dna origami. *Nano letters*, 18(1):405–411, 2018.
- [28] Felix Benz, Mikolaj K Schmidt, Alexander Dreismann, Rohit Chikkaraddy, Yao Zhang, Angela Demetriadou, Cloudy Carnegie, Hamid Ohadi, Bart De Nijs, Ruben Esteban, et al. Single-molecule optomechanics in "picocavities". *Science*, 354(6313):726–729, 2016.
- [29] Lukas A Jakob, William M Deacon, Yuan Zhang, Bart de Nijs, Elena Pavlenko, Shu Hu, Cloudy Carnegie, Tomas Neuman, Ruben Esteban, Javier Aizpurua, et al. Giant optomechanical spring effect in plasmonic nano-and picocavities probed by surface-enhanced raman scattering. *Nature Communications*, 14(1):3291, 2023.
- [30] Rohit Chikkaraddy, Bart De Nijs, Felix Benz, Steven J Barrow, Oren A Scherman, Edina Rosta, Angela Demetriadou, Peter Fox, Ortwin Hess, and Jeremy J Baumberg. Single-molecule strong coupling at room temperature in plasmonic nanocavities. *Nature*, 535(7610):127–130, 2016.
- [31] Gülis Zengin, Martin Wersäll, Sara Nilsson, Tomasz J Antosiewicz, Mikael Käll, and Timur Shegai. Realizing strong light-matter interactions between

- single-nanoparticle plasmons and molecular excitons at ambient conditions. *Physical review letters*, 114(15):157401, 2015.
- [32] Martin B Plenio, SF Huelga, A Beige, and PL Knight. Cavity-loss-induced generation of entangled atoms. *Physical Review A*, 59(3):2468, 1999.
- [33] S Hughes. Modified spontaneous emission and qubit entanglement from dipole-coupled quantum dots in a photonic crystal nanocavity. *Physical review letters*, 94(22):227402, 2005.
- [34] Sabrina Maniscalco, Francesco Francica, Rosa L Zaffino, Nicola Lo Gullo, and Francesco Plastina. Protecting entanglement via the quantum zeno effect. *Physical review letters*, 100(9):090503, 2008.
- [35] Francesco Francica, Sabrina Maniscalco, Jyrki Piilo, Francesco Plastina, and K-A Suominen. Off-resonant entanglement generation in a lossy cavity. *Physical Review A*, 79(3):032310, 2009.
- [36] Jiamin Hou, Karolina Słowik, Falk Lederer, and Carsten Rockstuhl. Dissipation-driven entanglement between qubits mediated by plasmonic nanoantennas. *Physical Review B*, 89(23):235413, 2014.
- [37] Mikhail Tokman, Alex Behne, Brandon Torres, Maria Erukhimova, Yongrui Wang, and Alexey Belyanin. Dissipation-driven formation of entangled dark states in strongly coupled inhomogeneous many-qubit systems in solid-state nanocavities. *Physical Review A*, 107(1):013721, 2023.
- [38] Diego Martin-Cano, Alejandro González-Tudela, Luis Martín-Moreno, FJ García-Vidal, Carlos Tejedor, and Esteban Moreno. Dissipation-driven generation of two-qubit entanglement mediated by plasmonic waveguides. *Physical Review B*, 84(23):235306, 2011.

- [39] Kalun Bedingfield, Benjamin Yuen, and Angela Demetriadou. Subradiant entanglement in plasmonic nanocavities. *arXiv preprint arXiv:2310.06462*, 2023.
- [40] Rui-Qi Li, D Hernánez-Pérez, FJ García-Vidal, and AI Fernández-Domínguez. Transformation optics approach to plasmon-exciton strong coupling in nanocavities. *Physical review letters*, 117(10):107401, 2016.
- [41] Ivan Medina, Francisco J García-Vidal, Antonio I Fernández-Domínguez, and Johannes Feist. Few-mode field quantization of arbitrary electromagnetic spectral densities. *Physical Review Letters*, 126(9):093601, 2021.
- [42] Zhicong He, Cheng Xu, Wenhao He, Jinhua He, Yunpeng Zhou, and Fang Li. Principle and applications of multimode strong coupling based on surface plasmons. *Nanomaterials*, 12(8):1242, 2022.
- [43] Yanji Yang, Rohit Chikkaraddy, Qianqi Lin, Daniel DA Clarke, Daniel Wigger, Jeremy J Baumberg, and Ortwin Hess. Electrochemically switchable multimode strong coupling in plasmonic nanocavities. *Nano letters*, 24(1):238–244, 2024.
- [44] Wei Yan, Rémi Faggiani, and Philippe Lalanne. Rigorous modal analysis of plasmonic nanoresonators. *Physical Review B*, 97(20):205422, 2018.
- [45] Philippe Lalanne, Wei Yan, Kevin Vynck, Christophe Sauvan, and Jean-Paul Hugonin. Light interaction with photonic and plasmonic resonances. *Laser & Photonics Reviews*, 12(5):1700113, 2018.
- [46] Philippe Lalanne. Light-in-complex-nanostructures/man: Versions 7.2 of qnmeig and qnmpole. <https://doi.org/10.5281/zenodo.5017292>, 2021.

- [47] Nuttawut Kongsuwan, Angela Demetriadou, Matthew Horton, Rohit Chikkaraddy, Jeremy J Baumberg, and Ortwin Hess. Plasmonic nanocavity modes: From near-field to far-field radiation. *ACS Photonics*, 7(2):463–471, 2020.
- [48] Kalun Bedingfield, Eoin Elliott, Arsenios Gisdakis, Nuttawut Kongsuwan, Jeremy J Baumberg, and Angela Demetriadou. Multi-faceted plasmonic nanocavities. *Nanophotonics*, 12(20):3931–3944, 2023.
- [49] William K Wootters. Entanglement of formation and concurrence. *Quantum Inf. Comput.*, 1(1):27–44, 2001.
- [50] Michael Walter, David Gross, and Jens Eisert. Multipartite entanglement. *Quantum Information: From Foundations to Quantum Technology Applications*, pages 293–330, 2016.

Acknowledgements (not compulsory)

AD gratefully acknowledges support from the Royal Society University Research Fellowship URF\R1\180097 and URF\R\231024, Royal Society Research grants RGS\R1\211093, funding from ESPRC grants EP/Y008774/1 and EP/X012689/1. AD, BY acknowledge support from Royal Society Research Fellows Enhancement Award RGF\EA\181038, and AD, AC acknowledge funding from EPSRC for the CDT in Topological Design EP/S02297X/1.

Author contributions statement

A.C. conducted the calculations, analysed the results, put the together the numerical codes and performed the analytical derivations. B.Y.assisted with the

theoretical methodology and code analysis and A.D. conceived the theoretical investigation on this topic. All authors reviewed the manuscript.

Additional information

The authors declare no competing interests.